



# City Research Online

## City St George's, University of London

**Citation:** Khan, S. & Ivanov, A. (1993). Calculation of static characteristics of linear step motors for control rod drives of nuclear reactors-an approximate approach. 1993 Sixth International Conference on Electrical Machines and Drives(376), pp. 523-528.

This is the accepted version of the paper.

This version of the publication may differ from the final published version. To cite this item please consult the publisher's version.

**Permanent repository link:** <https://openaccess.city.ac.uk/id/eprint/23736/>

**Copyright and Reuse:** Copyright and Moral Rights remain with the author(s) and/or copyright holders. Copies of full items can be used for personal research or study, educational, or not-for-profit purposes without prior permission or charge, unless otherwise indicated, provided that the authors, title and full bibliographic details are credited, a hyperlink and/or URL is given for the original metadata page and the content is not changed in any way. For full details of reuse please refer to [City Research Online policy](#).

## CALCULATION OF STATIC CHARACTERISTICS OF LINEAR STEP MOTORS FOR CONTROL ROD DRIVES OF NUCLEAR REACTORS - AN APPROXIMATE APPROACH

S H Khan     A A Ivanov

City University, London, UK  
St. Petersburg State Technical University, St. Petersburg, Russia

### ABSTRACT

This paper describes an approximate method for calculating the static characteristics of linear step motors (LSM), being developed for control rod drives (CRD) in large nuclear reactors. The static characteristic of such a LSM which is given by the variation of electromagnetic force with armature displacement determines the motor performance in its standing and dynamic modes. The approximate method of calculation of these characteristics is based on the permeance analysis method applied to the phase magnetic circuit of LSM. This is a simple, fast and efficient analytical approach which gives satisfactory results for small stator currents and weak iron saturation, typical to the standing mode of operation of LSM. The method is validated by comparing theoretical results with experimental ones.

### INTRODUCTION

Despite the Chernobyl accident, the contribution of atomic power plants in the total output of electric energy in many countries around the world is still rising. This intensive development of atomic energy and the tendency to increase the unit power output of reactors set the complex task of ensuring their safe, reliable and economic exploitation. This is accomplished by ensuring controllability of energy output locally as well as globally over the entire volume of the reactor core by suitably designing the CRD of nuclear reactors. Basically, it consists of movable control rods, made of neutron absorbing materials in the form of individual rods or group of rods (cassettes, clusters, etc.) and a driving mechanism to move them inside the reactor core [1-3]. The key element of this driving mechanism is the electric motor, upon the rational selection and reliable functioning of which, to a great extent depend the safety and reliability of the entire power plant. In recent years countries like Russia, USA, France, Germany and Italy are developing linear and discrete electromagnetic driving mechanisms for CRD with passive armature linear step motors [1-3]. These CRD with LSM are fast, highly reliable due to the simplicity of kinematics and accurate in the fixation of control rods.

One of the vital performance characteristics of LSM is the static characteristic which gives the variation of electromagnetic force produced by the motor with armature displacement. It determines motor performance in its standing (when the armature with

controls rods attached to it is held at a fixed position by electromagnetic force) and dynamic (when the armature is moved by sequential excitation of stator windings) modes of operation. In order to design reliable and economically viable CRD with LSM it is important to be able to calculate and evaluate their static characteristics. Although rotating step motors are well covered in literature, there are a few published papers which concern linear step motors [4, 5]. Two methods, approximate and accurate have been developed [6, 7] for the calculation of static characteristics of LSM. The approximate method, described in this paper is based on the permeance analysis approach [5, 8] and gives satisfactory results for small stator currents and low iron saturation. This is quite useful for the fast evaluation of motor performance at the earlier stages of their CAD without needing the computationally intensive modelling of magnetic fields by the finite element method on which the accurate method is based. The approximate method

was used to calculate the static characteristics of LSM designed by the researchers at "Ijorcki Javod" (St. Petersburg, Russia) for CRD (namely, linear synchronous electromagnetic drive, LSED) of large pressurised water reactors with electrical power output of 1000 MW (VVER-1000) and more [9, 10]. Some of the results are compared with experimental ones to establish the validity of the adopted approximate approach.

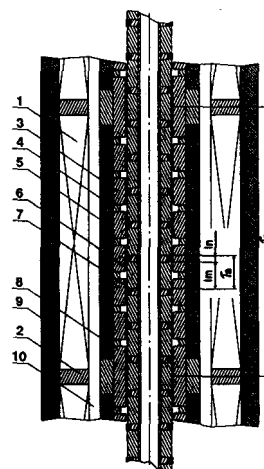


Figure 1. Longitudinal section of a phase of the LSM

### CONSTRUCTIVE FEATURES AND THE GEOMETRIC PARAMETERS OF A LSM

Figure 1 shows the longitudinal section of one of the phases of the 4-phase LSM designed at "Ijorcki Javod". It consists of the stator with cylindrical dc winding (1), poles (2) and ring elements in the form of

alternately arranged magnetic (3) and nonmagnetic (4) sleeves. The hermetically sealed cylinder (5) of the stator is made of nonmagnetic material (except the magnetic shunts under the poles) and withstands the high pressure inside the reactor vessel. The armature, in the form of a thin-wall hollow cylinder is made up of alternately arranged magnetic (6) and nonmagnetic (7) sleeves. These nonmagnetic sleeves are made up of the inner nonmagnetic ring and the outer ring made of antifriction material and acts as slide bearings. The height (length) of end (interphase) magnetic sleeves (8) of stator is higher than the height of those situated in between them (for example, 3). The outer casing of the motor (9) is made of magnetic material and acts as

TABLE 1 - Geometric parameters of LSM used in linear synchronous electromagnetic drives

Parameters	LSED	LSED-4
1. Internal diameter of the armature cylinder $D_{ci}$ , mm	23	23
2. Internal diameter of armature magnetic sleeves $D_{ai}$ , mm	30	30.1
3. External diameter of armature magnetic sleeves $D_{ae}$ , mm	49	54.7
4. Internal diameter of stator magnetic sleeves $D_{si}$ , mm	50	56.2
5. External diameter of stator magnetic sleeves $D_{se}$ , mm	76	76
6. Internal diameter of the cylindrical cooling duct $D_c$ , mm	no duct	94
7. Internal diameter of stator poles $D_p$ , mm	98	110
8. Width of stator poles $b_p$ , mm	16	16
9. Airgap between stator and armature $\delta$ , mm	0.5	0.75
10. Width of the cooling duct $\delta_c$ , mm	--	16
11. Thickness of the hermetically sealed cylinder of stator $\delta_s$ , mm	11	9
12. Height (length) of magnetic sleeves $l_m$ , mm	29	25
13. Height (length) of nonmagnetic sleeves $l_n$ , mm	7	7
14. Height (length) of end magnetic sleeves of stator $l_{mi}$ , mm	92	81
15. Number of phases in stator $m$	4	4
16. Number of nonmagnetic sleeves of stator per phase $n$	8	9

the outer magnetic circuit. The hollow cylindrical duct (10) in between the hermetically sealed cylinder (5) and stator windings (1) is meant for the circulation of water, cooling these windings. In reactors VVER-1000 the motor is designed to be mounted vertically on the lid of the reactor vessel. In case of power failure in the stator windings this ensures the armature with control rods to fall freely into the reactor core towards lowering its reactivity. Table 1 gives some of the geometric parameters of the LSM (shown in Figures 1 and 2) designed for two LSED. Some of the main design parameters of the motor are: armature step  $\tau_a = l_m + l_n$  and discrete step  $\tau_d = \tau_a/m$ . Discrete step  $\tau_d$  gives the armature displacement for unit voltage pulse in the stator winding. The height of the end magnetic sleeves of stator is chosen in such a way as to create a misalignment between stator and armature magnetic sleeves of adjacent phases. That is

$l_{mi} = l_m \pm \tau_d + k\tau_a = l_m + \tau_a(k \pm 1/m)$ , where  $k=0, 1, 2$ . For  $l_{mi}$  in Figure 2  $k=1$  and "+" sign is used before  $1/m$ . Phase step  $\tau_p$  (Figure 2) is given by the height of a phase,  $\tau_p = n\tau_a + l_m - l_n = \tau_a(n + k \pm 1/m)$ .

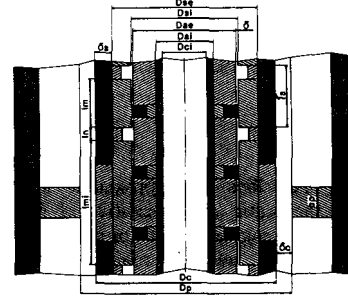


Figure 2. Various geometric parameters of the LSM

### WORKING PRINCIPLE AND THE STATIC CHARACTERISTIC OF THE LSM

With each voltage pulse current in the stator winding produces mmf  $F$  that gives rise to the magnetic flux  $\Phi = F/R(x) = FP(x)$ , where  $R(x)$  and  $P(x) = 1/R(x)$  are phase reluctance and permeance respectively. Armature movement changes the mutual alignments of stator and armature magnetic sleeves resulting in the change of reluctance  $R(x)$  and magnetic field energy  $W(x) = F\Phi/2 = F^2/2R(x) = F^2P(x)/2$ . These changes in energy  $W(x)$  give rise to electromagnetic force  $F(x)$  acting on the armature -

$$F(x) = \frac{dW(x)}{dx} = \frac{F^2}{2} \frac{d}{dx} \left( \frac{1}{R(x)} \right) = \frac{F^2}{2} \frac{dP(x)}{dx} \quad (1)$$

where  $x$  is the coordinate of armature displacement which characterises mutual alignments of stator and armature magnetic sleeves. Force  $F(x)$  acts in such a direction as to increase field energy  $W(x)$  and hence permeance  $P(x)$ . With armature movement,  $P(x)$  and so the force  $F(x)$  change periodically with a period of  $\tau_a$  so that  $F(x + \tau_a) = F(x)$ . Figure 3 shows how  $F(x)$  changes with coordinate  $x$  for a given phase. This is

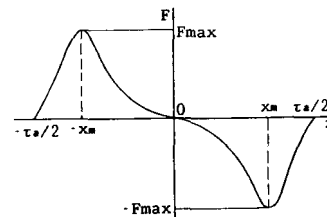


Figure 3. Static characteristic of the LSM

the static characteristic of the LSM shown in Figure 1.  $x=0$  in Figure 3 corresponds to a certain armature position when the central line through stator nonmagnetic sleeve aligns with that of the armature magnetic sleeve.  $F(x)$  attains its maximum for  $x = x_m$  when the armature and stator magnetic sleeve corners



nonmagnetic sleeves. Alternatively, this may be done by assuming probable flux paths for various armature positions  $x$ . For these, it is assumed that the flux distribution in the above regions of the inner magnetic circuit does not depend on the saturation of stator and armature magnetic sleeves. After plotting the respective flux paths permeances are calculated analytically for various  $x$ . The results of such calculations for the 4-phase LSM used in LSED are shown in Figures 7 and 8. Due to the symmetry in flux distribution in the inner magnetic circuit it is sufficient to consider  $0 \leq x \leq \tau_a/2$ . Figure 7 shows the variation of permeances  $P_1$  and  $P_2$  with armature displacement  $x$  which reflect the complex nature of flux distribution in the airgap for various positions of the armature. The

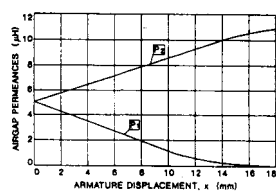


Figure 7. Variation of airgap permeances  $P_1$  and  $P_2$  with armature displacement  $x$

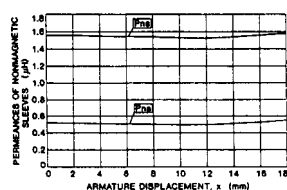


Figure 8. Variation of nonmagnetic sleeve permeances of stator ( $P_{ns}$ ) and armature ( $P_{na}$ ) with  $x$  constant

redistribution of flux components  $\Phi_s$ ,  $\Phi_a$  and  $\Phi_e$  with armature displacement  $x$  in the nonmagnetic sleeves is evident from the variation of permeances  $P_{ns}$  and  $P_{na}$  shown in Figure 8.

#### Calculation of Permeances Between the Armature and End Magnetic Sleeves of Stator

As said earlier the height of end magnetic sleeves of stator  $l_{m1}$  is different from that of other magnetic sleeves of stator and armature. This causes different flux distributions in the regions of end magnetic sleeves (shown schematically in Figure 9) for various

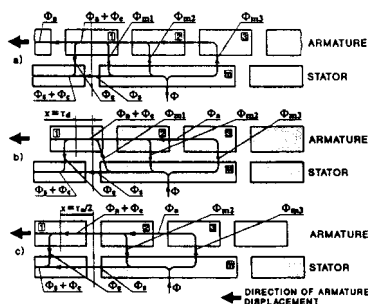


Figure 9. Flux distribution in the region of the first end magnetic sleeve used for the calculation of  $P_{e1}$

armature positions  $x$ . The total flux  $\Phi$  in the end magnetic sleeve  $m$  branches out into components  $\Phi_s$

which shunts through the stator sleeves, and  $\Phi_s + \Phi_e = \Phi_{m1} + \Phi_{m2} + \Phi_{m3}$  which crosses the airgap taking three parallel paths before entering the armature sleeves. From Figures 5 and 6 permeance  $P_{e1} = 1/R_{e1}$  is defined as the permeance between the end magnetic sleeve  $m$  and the armature magnetic sleeve closest to it (marked 1 in Figure 9) through which the flux  $\Phi_s + \Phi_e$  flows. As shown in Figure 9 armature magnetic sleeves marked 2 and 3 also take part in conducting this flux. Considering all these the magnetic circuit shown in Figure 9 may be represented by the equivalent circuit shown in Figure 10 which is used to calculate the permeance  $P_{e1}$ . For

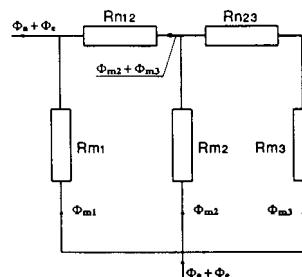


Figure 10. Equivalent circuit for the calculation of permeance  $P_{e1}$

this it is assumed that the reluctances of magnetic sleeves 2 and 3 are negligibly small since a very small amount of flux passes through them and, therefore their flux density is considerably smaller than the saturation density. The following symbols are used in Figure 10:  $R_{n12}$ ,  $R_{n23}$  - reluctances of nonmagnetic sleeves between 1, 2 and 2, 3 respectively (Figure 9);  $R_{m1}$ ,  $R_{m2}$ ,  $R_{m3}$  - airgap reluctances between  $m$  and 1, 2, 3 respectively. It may be assumed that  $R_{n12} = R_{n23} = R_{na} = 1/P_{na}$  and  $R_{m1} = R_1 = 1/P_1$ . Reluctances  $R_{m2}$  and  $R_{m3}$  are calculated from the following:

$$R_{m2} = \frac{\delta}{\pi\mu_0 l_m (D_{ae} + D_{si})/2} \quad (2)$$

$$R_{m3} = \begin{cases} \frac{\delta}{\pi\mu_0 (l_m - \tau_d + x)(D_{ae} + D_{si})/2}, & 0 \leq x \leq \tau_d \\ R_{m2} & \tau_d \leq x \leq \tau_a/2 \end{cases} \quad (3)$$

The variation of  $R_{m3}$  with armature displacement  $x$  is taken into account in equation (3). Knowing the above reluctances  $P_{e1}$  is calculated from the equivalent circuit in Figure 10 using -

$$P_{e1} = P_1 + \frac{1}{\frac{1}{\frac{1}{R_{m2}} + \frac{1}{R_{m3} + R_{na}}} + R_{na}} \quad (4)$$

Permeance due to the second end magnetic sleeve  $P_{e2}$  is calculated by considering the flux distribution in that region (see Figure 11). From the above this gives:

$$P_{e2} = P_2 + \frac{1}{\frac{1}{\frac{1}{R_{m2}} + \frac{1}{R_{m3} + R_{na}}} + R_{na}} \quad (5)$$

In equation (5) the reluctance  $R_{m3}$  is different from that given by equation (3) and is determined by taking

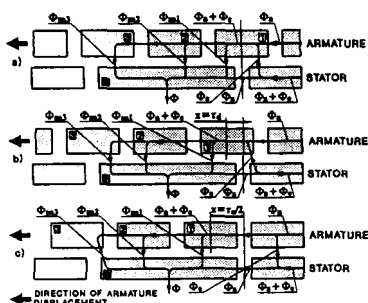


Figure 11. Flux distribution in the region of the second end magnetic sleeve used for the calculation of  $P_{e2}$

into account the variation of airgap reluctance with  $x$  between the magnetic sleeves  $m$  and  $3$  shown in Figure 11. Thus,

$$R_{m3} = \frac{\delta}{\pi\mu_0(lm - \tau_d - x)(Dae + Dsi)/2} \quad (6)$$

#### Iterative Calculation of the Reluctances of Magnetic Sleeves, Fluxes and Equivalent Phase Permeance

Reluctances of magnetic sleeves of stator and armature  $R_{ms}$  and  $R_{ma}$  are determined iteratively which lies in the basis of the approximate method of calculation of phase reluctance  $R$  (or permeance  $P$ ) and the static characteristics of LSM. For this, it is assumed that flux distributions in magnetic sleeves are uniform and, for a given alignment of stator and armature magnetic sleeves their permeabilities  $\mu_s$  and  $\mu_a$  depend only on the total flux passing through them and not on coordinate  $x$ . It is assumed that the variation of total flux in the magnetic sleeves with  $x$  determined by airgap flux  $\Phi_e$  is linear. From this the average calculated flux components in stator and armature magnetic sleeves  $\Phi_{sc}$  and  $\Phi_{ac}$  are given by  $\Phi_{sc} = \Phi_s + \Phi_e/2$  and  $\Phi_{ac} = \Phi_a + \Phi_e/2$ . The effective permeabilities  $\mu_s$  and  $\mu_a$  are calculated from the flux densities  $B_s$  and  $B_a$  determined by these flux components:  $B_s = \Phi_{sc}/S_{ms}$ ,  $B_a = \Phi_{ac}/S_{ma}$  where  $S_{ms}$  and  $S_{ma}$  are respectively the cross sectional areas of stator and armature magnetic sleeves. Now, from respective magnetisation curves  $\mu_s = B_s/H_s$  and  $\mu_a = B_a/H_a$  where  $H_s$ ,  $H_a$  are field intensities corresponding to  $B_s$  and  $B_a$ . Knowing  $\mu_s$  and  $\mu_a$  magnetic sleeve reluctances  $R_{ms}$  and  $R_{ma}$  are calculated:  $R_{ms} = lm/(\mu_s S_{ms})$  and  $R_{ma} = lm/(\mu_a S_{ma})$ .

Knowing  $R_{ms}$ ,  $R_{ma}$  and other reluctances phase reluctance  $R$ , total flux  $\Phi$  and its components  $\Phi_s$ ,  $\Phi_a$  and  $\Phi_e$  could be calculated from the equivalent circuit shown in Figure 6. But it is not possible to do that directly since  $R_{ms}$  and  $R_{ma}$  themselves depend on the total flux  $\Phi$ . For this reason the above calculation can be effectively done by successive iterations in

which the flux components  $\Phi_s$ ,  $\Phi_a$  and  $\Phi_e$  are determined by solving the following set of equations of mmf balance for these flux paths (Figure 6):

$$\begin{aligned} F &= \Phi R_{pe} + n\Phi_s R_{ns} + (n-1)(\Phi_s + \Phi_e/2)R_{ms} \\ F &= \Phi R_{pe} + (n-1)\Phi_a R_{na} + (\Phi_a + \Phi_e)(R_{e1} + R_{e2}) + \\ &\quad + n(\Phi_a + \Phi_e/2)R_{ma} \quad (7) \\ F &= \Phi R_{pe} + \Phi_e(n-1)(R_1 + R_2) + (\Phi_a + \Phi_e) \times \\ &\quad \times (R_{e1} + R_{e2}) + n(\Phi_a + \Phi_e/2)R_{ma} + \\ &\quad + (n-1)(\Phi_s + \Phi_e/2)R_{ms} \end{aligned}$$

For the iterative solution of (7) it is convenient to rewrite the equations in terms of flux components in the  $k$ -th iteration:

$$\begin{aligned} \Phi_s^{(k)} &= F_{ic}^{(k)}/R_s \\ \Phi_a^{(k)} &= F_{ic}^{(k)}/R_a \\ \Phi_e^{(k)} &= F_{ic}^{(k)}/R_e \quad (8) \end{aligned}$$

In the first iteration ( $k=1$ ) the mmf drop in the inner magnetic circuit  $F_{ic}$  in equation (8) is taken as  $F_{ic}^{(1)} = (0.8-0.9)F$  and in successive iterations  $F_{ic}^{(k)} = F - \Phi^{(k-1)}R_{pe}$ . Equivalent reluctances  $R_s$ ,  $R_a$  and  $R_e$  due to the flux paths  $\Phi_s$ ,  $\Phi_a$  and  $\Phi_e$  respectively are calculated in the first iteration by assuming that the reluctances of magnetic sleeves  $R_{ms} = R_{ma} = 0$ . This gives for  $k=1$

$$\begin{aligned} R_s^{(1)} &= nR_{ns} \\ R_a^{(1)} &= (n-1)R_{na} + 2(R_{e1} + R_{e2}) \\ R_e^{(1)} &= (n-1)(R_1 + R_2) + 2(R_{e1} + R_{e2}) \quad (9) \end{aligned}$$

and in successive iterations-

$$\begin{aligned} R_s^{(k)} &= nR_{ns} + (n-1)(1 + \Phi_e^{(k-1)}/2\Phi_s^{(k-1)})R_{ms}^{(k)} \\ R_a^{(k)} &= (n-1)R_{na} + (1 + \Phi_e^{(k-1)}/\Phi_a^{(k-1)})(R_{e1} + R_{e2}) + \\ &\quad + n(1 + \Phi_e^{(k-1)}/2\Phi_a^{(k-1)})R_{ma}^{(k)} \quad (10) \\ R_e^{(k)} &= (n-1)(R_1 + R_2) + (1 + \Phi_e^{(k-1)}/\Phi_a^{(k-1)}) \times \\ &\quad \times (R_{e1} + R_{e2}) + n(1 + \Phi_e^{(k-1)}/2\Phi_a^{(k-1)}) \times \\ &\quad \times R_{ma}^{(k)} + (n-1)(1 + \Phi_e^{(k-1)}/2\Phi_s^{(k-1)})R_{ms}^{(k)} \end{aligned}$$

The total flux  $\Phi^{(k)}$  in  $k$ -th iteration is calculated from its components determined in  $(k-1)$ -th iteration:

$$\Phi^{(k)} = \Phi_s^{(k-1)} + \Phi_a^{(k-1)} + \Phi_e^{(k-1)} \quad (11)$$

In each iteration, starting from the 2nd before the calculation of reluctances  $R_s^{(k)}$ ,  $R_a^{(k)}$  and  $R_e^{(k)}$  in the  $k$ -th iteration magnetic sleeve reluctances  $R_{ms}^{(k)}$  and  $R_{ma}^{(k)}$  are calculated using the flux components  $\Phi_s^{(k-1)}$ ,  $\Phi_a^{(k-1)}$  and  $\Phi_e^{(k-1)}$  determined in the  $(k-1)$ -th iteration. For this the procedure described at the beginning of this section for calculating  $R_{ms}$  and  $R_{ma}$  from  $\mu_s$  and  $\mu_a$  using the flux components  $\Phi_{sc}$  and  $\Phi_{ac}$  is used. However, theoretical experiments show that the above method for updating the permeabilities can diverge the iterative process. To avoid this and to accelerate convergence the permeabilities of magnetic sleeves are corrected in each  $k$ -th iteration using

$$\begin{aligned} \mu_s^{(k)} &= q(B_s^{(k)}/H_s^{(k)} + (1-q)\mu_s^{(k-1)}) \\ \mu_a^{(k)} &= q(B_a^{(k)}/H_a^{(k)} + (1-q)\mu_a^{(k-1)}) \quad (12) \end{aligned}$$

where relaxation factor  $0.5 \leq q \leq 0.8$  and initially  $\mu_s^{(1)} = \mu_a^{(1)} = 100\mu_0$ . The above iterative process is ended when the flux components in two successive iterations become very close. For this the following end condition can be used:

$$|\Phi_s^{(k)}/\Phi_s^{(k-1)} - 1| + |\Phi_a^{(k)}/\Phi_a^{(k-1)} - 1| + |\Phi_e^{(k)}/\Phi_e^{(k-1)} - 1| + |\Phi/\Phi^{(k-1)} - 1| \leq \epsilon \quad (13)$$

where  $\epsilon$  is the end factor determined by accuracy requirements. Thus, using the method described above the total flux  $\Phi(x)$  is calculated for various armature displacements  $x$  from which phase permeance  $P(x) = \Phi(x)/F$  is calculated. Finally, electromagnetic force  $F(x)$  is calculated as a function of  $x$  by differentiating  $P(x) = f(x)$  using equation (1).

## RESULTS AND DISCUSSIONS

Some of the results of above calculations for the 4-phase LSM used in LSED are presented in Figures 12 and 13. Figure 12 shows the variation of phase permeance with armature displacement for a small

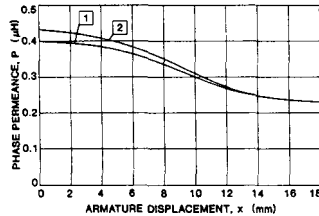


Figure 12. Variation of phase permeance  $P$  with armature displacement  $x$ : 1 - considering saturation effects, 2 - without considering saturation effects

stator current  $I = 5$  A with (1 -  $P_s(x)$ ) and without (2 -  $P_{uns}(x)$ ) saturation of magnetic sleeves taken into account. For  $P_{uns}(x)$  it is assumed that  $\mu_s = \mu_a = \infty$  and hence,  $R_{ms} = R_{ma} = 0$ . As can be seen from Figure 12 the effect of saturation on phase permeance for small stator current is not significant. Figure 13

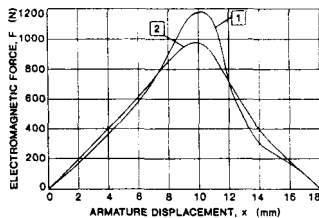


Figure 13. Static characteristics of the LSM: 1 - approximate method, 2 - experimental

shows the static characteristic of the LSM calculated by the approximate method (1) for  $I = 5$  A and its comparison with the experimental characteristic (2) obtained from [10]. It shows, in general satisfactory agreement which validates the above described method. Maximum error of about 15% can be seen in

the region of highest electromagnetic force for  $x \approx 11$  mm. This is due to the approximate incorporation of iron saturation, especially the saturation of magnetic sleeve corners which takes place (even for small currents) for certain armature positions for which stator and armature magnetic sleeve corners align opposite to each other.

## CONCLUSIONS

A method has been developed for the approximate calculation of static characteristics of linear step motors which gives satisfactory results for small currents and weak iron saturation. This is a simple and fast analytical technique which can be readily used at the early stages of CAD of these motors to generate, verify and evaluate initial designs.

## REFERENCES

- [1]. Emelianov, I. Y., Voscoboinikov, V. V., and Maslionok, B. A., 1987, "Fundamentals of Construction of Control Rod Drive Mechanisms in Nuclear Reactors", Energoatomizdat, Moscow, Russia (in Russian)
- [2]. Emelianov, I. Y., Voscoboinikov, V. V., and Maslionok, B. A., 1978, "Fundamentals of Design of Control Mechanisms in Nuclear Reactors", Atomizdat, Moscow, Russia (in Russian)
- [3]. Patent, France no. 2526241, Int. Cl. H02K 41/03, 1982
- [4]. Schoorens, H., Guegan, Y., and Favier, P., 1984, *Proc. Int. Conf. Electrical Machines*, 2, 559-562
- [5]. Hirata, K., Kagami, Y., Yanosaka, M., Ishihara, Y., and Todaka, T., 1992, *IEEE Trans. Magn.*, 28, 1394-1397
- [6]. Khan, S. H., 1987, "Development of the Methods of Calculation of Magnetic Fields and Static Characteristics of Linear Step Motors for Control Rod Drives of Nuclear Reactors", Ph.D Thesis, St Petersburg State Technical University, St. Petersburg, Russia (in Russian)
- [7]. Khan, S. H., and Ivanov, A. A., 1992, *IEEE Trans. Mag.*, 28, 2277-2279
- [8]. Zhu, Z. Q., and Howe, D., 1992, *IEEE Trans. Mag.*, 28, 1371-1374
- [9]. Zavalova, G. I., Ivanov, I. V., and Nikolaev, V. P., 1982, "Linear Step Motor", patent USSR no. 920977, Int. Cl. H02K 41/035, H02K 37/00
- [10]. "Investigation of the Model of Electromagnet of Linear Step Motor", 1979, Intermediate Report of the Industry G-4781, no. 1802.40.91.500 D1, St. Petersburg, Russia (in Russian)